Title
Pitted terrains on (1) Ceres and implications for shallow subsurface volatile distribution.

Journal
Geophysical research letters, 44(13)

ISSN
0094-8276

Authors
Sizemore, HG
Platz, T
Schorghofer, N
et al.

Publication Date
2017-07-01

DOI
10.1002/2017gl073970

Peer reviewed

AGU PUBLICATIONS

Geophysical Research Letters

RESEARCH LETTER
10.1002/2017GL073970

Key Points:
- Fresh complex craters on Ceres host distinctive pitted terrains that are morphologically similar to pitted materials on Mars and Vesta
- Pitted terrains on Ceres likely form via the rapid volatilization of molecular H_2O entrained in impact materials
- Pitted terrains may be common morphological markers of volatile-rich near-surface material in the asteroid belt

Supporting Information:
- Supporting Information S1
- Supporting Information S2

Correspondence to:
H. G. Sizemore,
sizemore@psi.edu

Citation:
Sizemore, H. G., et al. (2017), Pitted terrains on (1) Ceres and implications for shallow subsurface volatile distribution, *Geophys. Res. Lett.*, *44*, 6570–6578, doi:10.1002/2017GL073970.

Received 26 APR 2017
Accepted 22 JUN 2017
Accepted article online 27 JUN 2017,
Published online 15 JUL 2017

Pitted terrains on (1) Ceres and implications for shallow subsurface volatile distribution

H. G. Sizemore[1], T. Platz[2], N. Schorghofer[1], T. H. Prettyman[1], M. C. De Sanctis[3], D. A. Crown[1], N. Schmedemann[4], A. Neesemann[4], T. Kneissl[4], S. Marchi[5], P. M. Schenk[6], M. T. Bland[7], B. E. Schmidt[8], K. H. G. Hughson[9], F. Tosi[3], F. Zambon[3], S. C. Mest[1], R. A. Yingst[1], D. A. Williams[10], C. T. Russell[9], and C. A. Raymond[11]

[1]Planetary Science Institute, Tucson, Arizona, USA, [2]Max Planck Institute for Solar System Research, Göttingen, Germany, [3]Istituto di Astrofisica e Planetologia Spaziali, INAF, Rome, Italy, [4]Department of Earth Sciences, Freie Universität Berlin, Berlin, Germany, [5]Southwest Research Institute, Boulder, Colorado, USA, [6]Lunar and Planetary Institute, Houston, Texas, USA, [7]USGS Astrogeology Science Center, Flagstaff, Arizona, USA, [8]Department of Planetary and Space Physics, Georgia Institute of Technology, Atlanta, Georgia, USA, [9]Department of Earth, Planetary, and Space Sciences, University of California Los Angeles, Los Angeles, California, USA, [10]School of Earth and Space Sciences, Arizona State University, Tempe, Arizona, USA, [11]Jet Propulsion Laboratory, California Institute of Technology, Pasadena, California, USA

Abstract Prior to the arrival of the Dawn spacecraft at Ceres, the dwarf planet was anticipated to be ice-rich. Searches for morphological features related to ice have been ongoing during Dawn's mission at Ceres. Here we report the identification of pitted terrains associated with fresh Cerean impact craters. The Cerean pitted terrains exhibit strong morphological similarities to pitted materials previously identified on Mars (where ice is implicated in pit development) and Vesta (where the presence of ice is debated). We employ numerical models to investigate the formation of pitted materials on Ceres and discuss the relative importance of water ice and other volatiles in pit development there. We conclude that water ice likely plays an important role in pit development on Ceres. Similar pitted terrains may be common in the asteroid belt and may be of interest to future missions motivated by both astrobiology and in situ resource utilization.

1. Introduction

The Dawn spacecraft entered orbit around dwarf planet Ceres on 5 March 2015. Over the first 16 months at Ceres, the spacecraft obtained morphological, topographical, mineralogical, elemental, and gravity data from a series of successively lower orbits. Framing Camera (FC) images from high altitude mapping orbit (HAMO) and low altitude mapping orbit (LAMO) have provided global coverage of Ceres' surface at pixel scales of 140 m/pixel and 35 m/pixel, respectively. In the FC data set we have identified distinct pitted terrains, characterized by clusters of round-to-irregular, apparently rimless pits in smooth impact materials. We describe the morphology, setting, and geographic distribution of these terrains, which exhibit striking similarities to pitted materials previously discovered by Dawn at Vesta [*Denevi et al.*, 2012; *Reddy et al.*, 2012] and pitted materials identified in low- and middle-latitude Martian craters [*Tornabene et al.*, 2012; *Boyce et al.*, 2012]. We discuss likely formation mechanisms for the Cerean pitted materials, as well as implications for the geographic distribution and concentration of shallow volatiles on Ceres.

2. Methods

Prior to Dawn's arrival at Ceres it was anticipated that the dwarf planet's outer shell might be water ice-rich [e.g., *McCord and Sotin*, 2005, and references therein]. Further, thermal simulations predicted that ice in the shallow subsurface could be protected against sublimation on billion year timescales by a dry silicate lag, varying in depth from tens or hundreds of meters near the equator to centimeters near the pole [e.g., *Fanale and Salvail*, 1989; *Schorghofer*, 2008, 2016]. Using FC images, we have carried out global searches for morphological features that are potentially diagnostic of the presence of subsurface ice based on analogies with a variety of solar system objects [e.g., *Schmidt et al.*, 2017]. Features of particular interest in this search were pits and depressions, which have been linked to gas-phase volatile loss on Mars, Callisto, Europa, Mercury, Vesta, Triton, and Pluto. We carried out a global search for pits and depressions during each mapping orbit (Survey, HAMO, and LAMO). Because Ceres' surface morphology is dominated by impact structures, distinguishing between features produced by volatile loss and features produced by primary

and secondary impacts was an ongoing consideration in our analysis of FC data. Our criteria for identification of pits, depressions, and pit clusters relevant to volatiles were the presence of (1) rimless depressions, with (2) round-to-irregular, elongate, branching, or polygonal margins, and exhibiting (3) overlapping or repeating patterns. These criteria were based primarily on characteristics of the Martian "Swiss Cheese" and dissected mantle terrains [*Malin et al*., 2001; *Milliken and Mustard*, 2003; *Byrne and Ingersoll*, 2003], the morphology of pitted materials inferred to be volatile-rich in craters on Vesta, Mars, and Mercury [*Denevi et al*., 2012; *Tornabene et al*., 2012; *Blewett et al*., 2011], and reviews of ice sublimation as a geomorphic process [e.g., *Mangold*, 2011; *Moore et al*., 1996]. Following completion of our global searches, we interpreted the nature of identified pits and depressions based on morphological comparisons to other solar system bodies and established numerical models of near-surface volatile transport [*Boyce et al*., 2012; *Schorghofer*, 2016].

3. Results

In the course of our global searches, we identified four regions with pits that met our criteria in LAMO images and three additional areas with ambiguous depressions potentially consistent with our criteria. All pitted terrains identified in LAMO data were associated with relatively fresh craters, prompting us to carry out focused repeat searches for pitting in all the most pristine Cerean craters. The results of these searches are summarized in Table 1 and Figure 1 and described in detail below.

Ikapati, Dantu, Haulani, and Kupalo craters exhibit clusters of pits that are distinguishable from nearby small impact craters, based on their lack of high standing rims, their rounded but irregular margins, and their tendency to occur in overlapping clusters on otherwise smooth, lightly cratered terrain. Ikapati and Dantu craters host the most extensive pit clusters on Ceres (Figure 2). Pits occur on floor materials and in smooth ejecta exterior to the crater rim at both locations. Pits exhibit a range of depths within individual clusters (typically tens of meters but extending to depths $>$150 m in the largest examples), and are generally conical or fluted in profile, rather than flat-floored. In the interior of Ikapati crater (depth 4 km, diameter 50 km) multiple clusters are distributed across smooth flat-lying material in the southeastern half of the crater (Figure S1 in the supporting information) [*Preusker et al*., 2016]. Exterior to Ikapati, pit clusters are present in the smooth ejecta ponded in topographic lows associated with preexisting large craters. Pit clusters on the Ikapati ejecta consist of smaller individual depressions than those in the crater interior. Individually, these smaller pits (diameters $<$0.5 km) are less easily distinguished from comparably sized impact craters because their margins/rims are not resolved; however, the pits appear incised in surrounding smooth impact material and their clustering on ponded material is texturally distinctive from impact craters.

The distribution and morphology of pits at Dantu (depth 4 km, diameter 126 km: Figure S3) is similar to Ikapati. Smooth deposits cover most of the Dantu floor, and smooth ejecta is ponded in topographic lows to the southwest of the Dantu rim. We identified pit clusters in both interior and exterior smooth material. As in Ikapati, the largest pits associated with Dantu (0.4 to 0.9 km) occur in the crater interior on smooth fill material; pits on ejecta materials are smaller (typically $<$0.3 km). Pits in the Dantu interior are clustered around the central peak/ring complex and smooth materials on the crater floor. Small impact craters, defined by their round shape and raised rims, are more abundant in the Dantu region than at Ikapati. The higher-background crater density and the prevalence of individual pits with diameters much smaller than 1 km makes distinction between "pits" and impact craters more ambiguous at Dantu than at Ikapati, particularly external to the Dantu rim.

The smooth floor material of Haulani crater (depth 2.5–3 km, diameter 34 km; Figure S2) is extensively pitted. Individual pits are $<$70 to ~400 m in diameter, tens of meters deep and exhibit the same morphological characteristics as those in Dantu and Ikapati. In Haulani, pit clusters are adjacent to and sometimes superposed by lobate and sinuous mass-wasting features sourced from the crater walls. Other pits are incised in materials that have flowed outward from the central peak complex, superposing other pitted materials on the southern crater floor. In the northwest quadrant of the crater, pits and floor fractures occur in close proximity [*Buczkowski et al*., 2016a]. Exterior to Haulani, much of the ejecta is extensively fluidized, with material that is smooth, sinuous, and exhibits localized lobate margins and ponding (Figure S2); however, we did not identify any pits or pit clusters on the Haulani ejecta.

Kupalo crater (depth 2.5 km, diameter 26 km; Figure S4) provides the final example of unambiguous pitting on Ceres. Kupalo is flat floored and hosts extended pit clusters, with a distribution similar to that seen on the Haulani floor. In the crater interior, pit clusters and/or pitted texture in otherwise smooth material are

Table 1. Summary of Pit Occurrence in Well-Preserved Impact Craters[a]

Parent Crater	Latitude	Longitude	Depth (km)	Diameter (km)	Pits?	Max Pit Diameter (m)	Approx. Crater Age (ma)	Pit Setting
Urvara	−45.66	249.24	5 to 6	170	degraded	2054.8	130–240 (−8/+20) Ma	smooth floor
Dantu	24.3	138.23	~4	126	abundant	1102.8	72–150 (−4/+9) Ma	smooth floor and ejecta
Occator	19.82	239.33	~4	92	few, ambiguous		21 (±0.4) Ma	wall terrace and ejecta
Ikapati	33.8	45.61	~4	50	abundant	866.5	19–43 (−2/+10) Ma	smooth floor and ejecta
Azacca	−6.66	218.4	~2.5	49	few, degraded	742.1	76 (±10) Ma	smooth floor
Haulani	5.8	10.77	2.5 to 3	34	abundant	372.9	1.7–2.7 (−0.2/+0.7)	smooth floor
Kupalo	−39.44	173.2	~2.5	26	abundant	326.2	<4.5 Ma (difficult to date)	smooth floor
Juling	−35.9	168.48	~1.75	20	none		<2.5 Ma (difficult to date)	
Oxo	42.21	359.6	<1	10	none		0.51 (±0.2) Ma	

[a]Crater age estimates are based on the Lunar Derived System (LDM) and are discussed in detail by *Schmedemann et al.* [2017] and *Williams et al.* [2017]. Pit diameters are determined via the technique described by *Kneissl et al.* [2011].

associated with sinuous, lobate, and streamlined patterns. We did not identify pit clusters or pitted textures in the Kupalo ejecta, despite its smooth texture, sinuosity, ponding, and lobate margins.

Our global search also revealed three less pristine craters, Urvara, Azacca, and Occator in which there is possible evidence of degraded pits. In the Urvara (depth 5–6 km, diameter 170 km) interior, two groups of hummocky depressions dissect the smooth floor material where the smooth material abuts the rough, high-standing central peak material. Scrutiny of the Urvara floor in LAMO images revealed that there are few distinct, steep-walled pits in either region. Instead, these areas consist of muted overlapping depressions with sloped walls and variable depths; the boundaries between individual depressions do not rise to the elevation of the surrounding terrain. The setting of this terrain is similar to pitted areas in the Dantu, Haulani, and Kupalo interiors. Exterior to Urvara, ejecta materials are too degraded to allow for a meaningful assessment of whether pits are present.

Azacca crater (depth 2.5 km, diameter 49.9 km) may also show evidence of degraded pits, although features at this location are much more ambiguous. The large-scale morphology of the crater is broadly similar to both Ikapati and Dantu; the density of superposed craters is much higher. Azacca is a flat-floored crater, with a central peak and prominent floor fractures. We identified two clusters of irregular, interconnected depressions and a single large isolated depression with irregular margins (~1 km by 400 m) on the Azacca floor (Figures S7c–S7f). Their setting and sizes are similar to pits identified elsewhere. We also observed a small number of ambiguous depressions on terrace material in Occator Crater (depth 4 km; diameter 92 km; Figure S6), but not on the extensively modified crater floor. The possible presence of degraded pits in less-pristine craters suggests that pits may be a common feature of fresh Cerean impact materials but that subsequent small impacts and mass wasting rapidly obscure them.

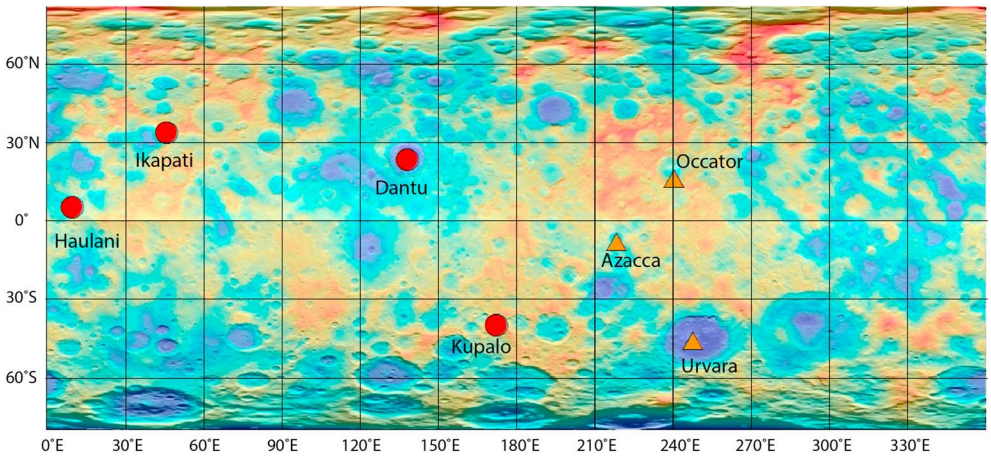

Figure 1. Global distribution of pitted crater materials on Ceres. Pitted materials similar to those identified in Vestan and Martian impact craters [*Denevi et al.*, 2012; *Tornabene et al.*, 2012] have been identified in Ikapati, Haulani, Dantu, and Kupalo craters (red circles) on Ceres. Depressions in Urvara, Occator, and Azacca may be degraded pits (orange triangles).

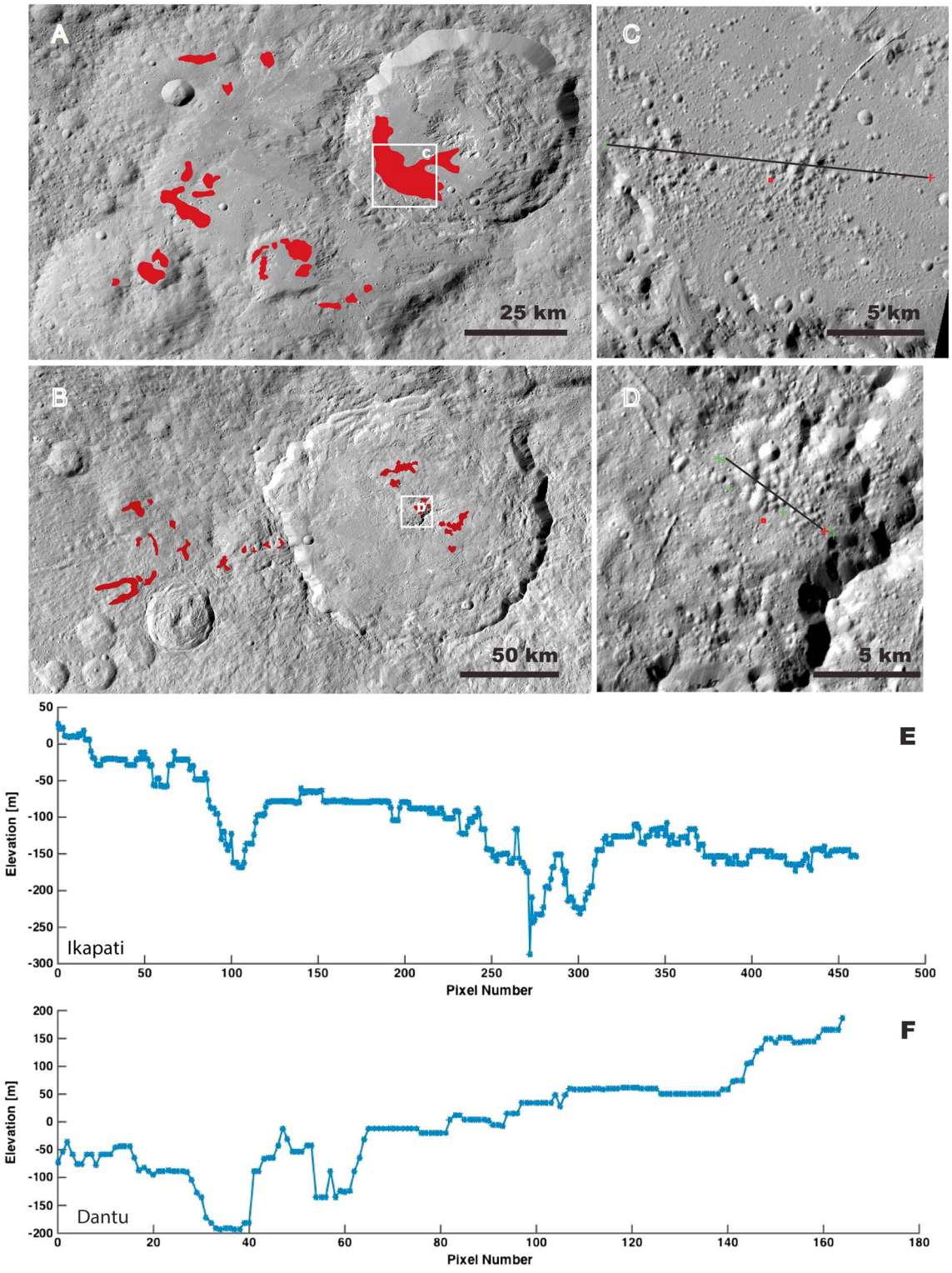

Figure 2. Pit images and topographic profiles in (a, c, and e) Ikapati and (b, d, and f) Dantu. Images are excerpted from a global LAMO mosaic provided by DLR. Topographic profiles are derived from stereo pairs of LAMO images using ISIS image processing software [*Becker et al.,* 2015].

Two prominent fresh craters, Juling and Oxo, show no evidence of pits. Juling (depth 1.75 km, diameter 20 km) is notable for its proximity to Kupalo, its near-complete lack of superposed craters, and its lobate ejecta and interior mass-wasting features. Juling is infilled by hummocky-to-lobate material, and lacks both

a flat floor and identified pits. Oxo (depth < 1 km, diameter 10 km) is similar to Juling in terms of size, lack of superposed impacts, and the presence of extensive lobate features interior and exterior to the crater rim. The Oxo materials include extensive bright deposits, and Oxo is one of two locations on Ceres for where there is spectral evidence of small quantities of water ice exposed at the surface [*Combe et al*., 2016]. The absence of superposed impact craters makes the nondetections at both Juling and Oxo unambiguous within the limits of LAMO image resolution, but does not rule out the presence of pits <60 m in diameter.

The morphology and setting of Cerean pitted terrains are remarkably similar to pitted terrains identified on Vesta and Mars and described by *Tornabene et al.* [2012] and *Denevi et al.* [2012] (Figures 3a–3c). At Ceres, Vesta, and Mars, individual pits have conical or fluted depth profiles, appear rimless (see discussion by *Tornabene et al.* [2012]) and/or overlap with adjacent pits forming shared boundaries. On all three planetary bodies, pits are associated with pristine craters, and degraded examples are seen in less pristine craters, suggesting that they are rapidly degraded. Individual pits and pit clusters are incised in smooth crater fill and ejecta materials. Commonly, this smooth material shows localized or pervasive evidence of flow—e.g., embayment relationships with high-standing terrain, lobate margins, streamlining, and/or ponding in topographic lows. At Haulani and Kupalo, as in Tooting Crater on Mars, pits occur on and are overprinted by lobate flows. On Ceres, as on Mars and Vesta, the largest pits and the densest concentrations of pits occur in the central portions of the smooth crater fill deposit, and/or along the contact between pitted materials and the bed rock of the central uplift (see Cerean examples in Figures S2–S5). In complex Martian craters, the densest clusters of pits occur on the lowest elevation surfaces in the crater interior and at locations where there are minimal effects of slumping and terracing; on Ceres Ikapati and Urvara exhibit similar trends. On Mars, Vesta, and Ceres, pit clusters are sometimes associated with or crosscut by fractures similar to fractures observe in large lunar craters [*Heather and Dunkin*, 2003; *Tornabene et al*., 2012; *Denevi et al*., 2012; *Buczkowski et al*., 2016b]. On Mars and Vesta, smaller pits occur where ejecta is ponded on terraces or in topographic lows exterior to the source crater. On Ceres, we see a clear example of the latter at Ikapati and a possible example of the former at Occator. Finally, the Cerean pits—like their Martian and Vestan counterparts—obey a power law-relating pit diameter to host crater diameter [*Tornabene et al*., 2012; *Denevi et al*., 2012] (Figure S8).

There are some limitations to the parallels that can be drawn between the pitted materials on the three bodies. *Denevi et al.* [2012] reported a distinctive thermal signature associated with the Vestan pitted terrains. Some Martian craters with pitted materials have characteristic thermal signatures, others do not [*Malin and Edgett*, 2001; *Tornabene et al*., 2006; *Preblich et al*., 2007; *Tornabene et al*., 2012]. We did not find a thermal signature associated with the Cerean pits (Figure S12) [*Capria et al*., 2014; *Tosi et al*., 2014]. The relatively low resolution of FC LAMO images at Ceres (35 m/pixel versus 17 m/pixel at Vesta) prevents the detailed analysis of individual pit morphology carried out by *Tornabene et al.* [2012] at Mars (HiRISE images have pixel scales of ~28 cm/pixel). Image resolution also introduces ambiguity in the identification of individual Cerean pits as distinct from small craters at locations where pits are small and/or background crater densities are high. However, the numerous parallels in morphology and setting between Cerean, Vestan, and Martian pitted materials suggest that the features on all three bodies are analogous and likely share a common formation process.

4. Discussion

On Mars, *Tornabene et al.* [2012] and *Boyce et al.* [2012] attributed the distinct morphology and distribution of pitted materials to the rapid devolatilization of impact materials following crater formation. *Denevi et al.* [2012] reached similar conclusions for Vesta. We also prefer a rapid postimpact formation model at Ceres, on physical and morphological grounds. Long-term sublimation of ground ice—a physical process commonly linked to the development of rimless pits and depressions—is *unlikely* to be responsible for pit production on Ceres for two reasons. First, modeled H_2O sublimation rates for Ceres are too slow to produce the observed relief during the short time since the formation of the host craters. We observe pits >100 m deep in craters that formed in the last 100 Myr (Table 1). We carried out simulations to determine the maximum relief that could be produced by sublimation of ground ice over the past Gyr on Ceres, and found it to be less than 4 m (Figure S9) [*Schorghofer*, 2016; *Rivkin et al*., 2010]. Second, no identified class of solar system morphological features produced by long-term sublimation is analogous to the Cerean pits. "Hollows" on Mercury have limited similarities (length scale and crater floor setting), but hollows are elongate,

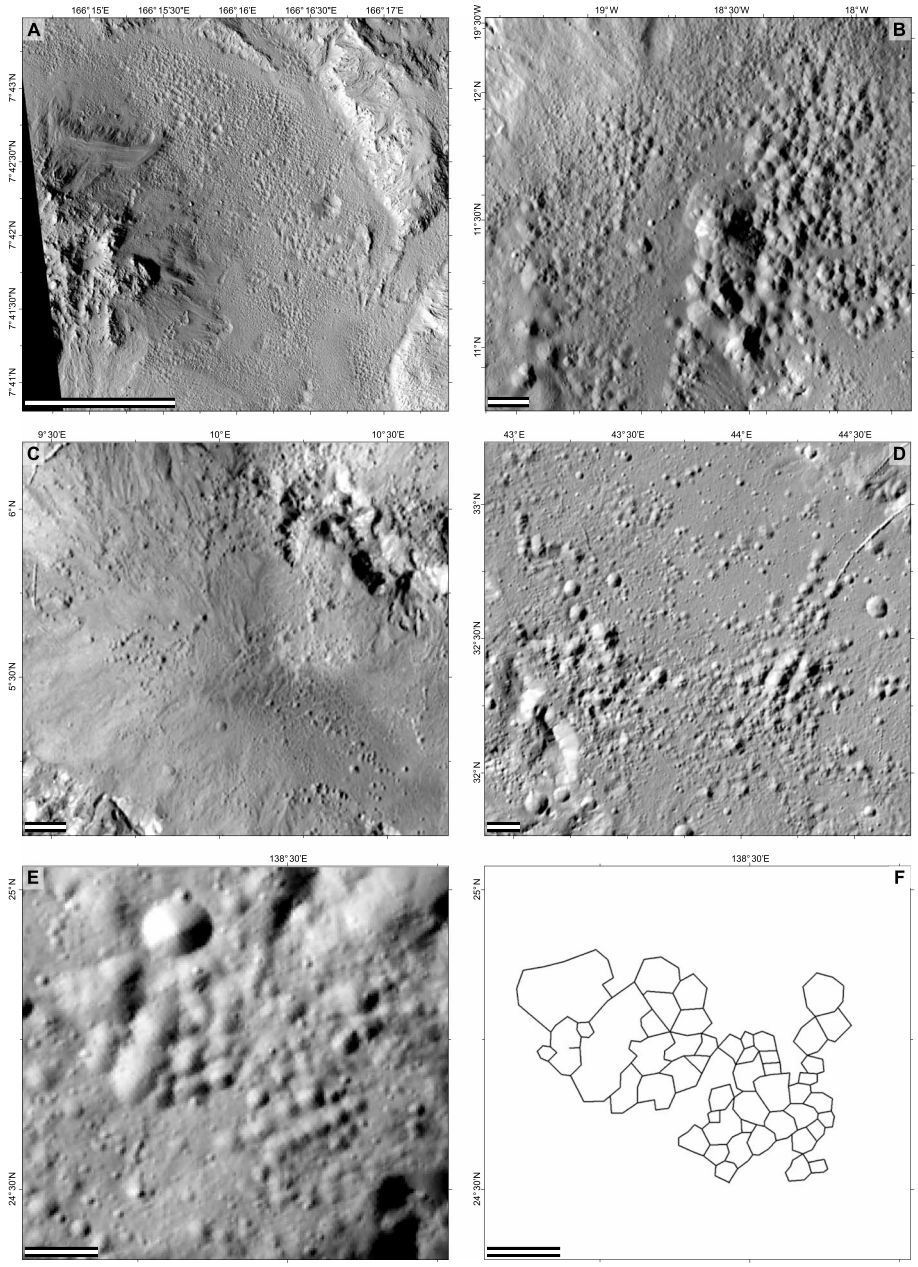

Figure 3. Comparison of pitted terrains on Mars, Vesta, and Ceres. (a) Pitted terrain within the 10.3 km diameter Zunil Crater (7.70°N/166.19°E) on Mars as seen in HiRISE image ESP_038250_1880 (0.25 m/pixel). (b) Pitted terrain within the 67.6 km diameter Marcia Crater (8.98°N/339.55°E) on Vesta as seen in Framing Camera images 14,662 (19.7 m/pixel). Pitted terrains observed on Ceres are highlighted in (c) Haulani Crater, (d) Ikapati Crater, and (e) Dantu Crater; Framing Camera nadir mosaic (30 m/pixel). (e) Lines indicating the shared borders of the Dantu pits; see Figure 3 of *Boyce et al.* [2012] for comparison. Scale bar indicates 1 km in all images. Note that north is *not* up.

branching, flat-floored, associated with bright halos, and occur in degraded craters [*Blewett et al.*, 2011] (Figure S10). The Cerean pit clusters, like the Martian pitted materials described by *Tornabene et al.* [2012], also exhibit limited similarities to ablation hollows or suncups [cf., *Mangold*, 2011], but there is no evidence for the extensive, nearly pure surface ice deposits required for suncup development on Ceres.

Boyce et al. [2012] developed conceptual and physical models for the development of Martian pitted materials, based on observations at Ries crater, Germany [*McEwen et al.*, 2007; *Tornabene et al.*, 2007, 2012; *Mouginis-Mark and Garbeil*, 2007; *Morris et al.*, 2010]. In the Boyce conceptual model, melt-bearing impact breccia with

entrained volatiles is deposited in a crater floor and on the surrounding terrain soon after an impact. Water vapor begins to escape from the deposit and establishes a series of preferential pathways that transport vapor and fine-grained material to the surface. Increased flow velocities form larger vent pipes and draw in additional gas via the Venturi effect. Flowing gas and entrained clasts erode the vent walls. Patterns of regularly spaced pits with subtle shared rims are left when the gas supply is depleted. This conceptual model explains the shape of individual pits, their occurrence in clusters, and the relationships between crater diameter, pit location, and pit size observed on Mars, Vesta, and Ceres (Figure 3).

The ultimate source of the pit-forming gas on Ceres is a matter of some interest for evaluating pre-Dawn predictions of abundant shallow ice. *Boyce et al.* [2012] estimated that low-latitude Martian target materials likely contain 4–10 wt % water in the form of pore space ice, and an additional ~4–7 wt % water bound in minerals. Based on the assumption that gas pressures in the melt-bearing layer should equal or exceed the overburden pressure to drive flow, *Boyce et al.* [2012] calculated outflow velocities that would exhaust the H_2O supply in the days immediately following the impact. They emphasized that the volatile supply might be exhausted on shorter timescales due to gas flow exploiting preferred pathways once Venturi pipes were established. Applying the *Boyce et al.* [2012] numerical model of pit-forming gas flow to Ceres (Figure S10) suggests that flow velocities and the time frame for pit formation are broadly comparable on Ceres and Mars; however, the total mass of H_2O required for pit development is smaller on Ceres than on Mars, due to Ceres' lower gravitational acceleration.

Is the gas driving Cerean pit development sourced from ground ice? *Denevi et al.* [2012] estimated that water bound in exogenic chondritic material was sufficient to produce pitted materials on Vesta, which is not thought to have endogenic sources of water. *Scully et al.* [2015] subsequently suggested a role for small quantities of ice. In contrast to Vesta, Ceres likely hosts substantial endogenic volatiles. Data from the Gamma Ray and Neutron Detector (GRaND) are broadly consistent with predictions of thermal stability models, which indicate that ice should be present in regolith pore spaces at depths of centimeters near the poles (inside the depth range of GRaND sensitivity) and depths of a few meters near the equator (not detectable by GRaND) [*Schorghofer*, 2016; *Prettyman et al*., 2017]. GRaND data also suggest that bound "water" (molecular H_2O, hydroxides, and hydroxyl groups) is present in the "dry" equatorial regolith at decimeter depth scales [*Prettyman et al*., 2017]. Data from the Visible and InfraRed Mapping Spectrometer (VIR-MS) indicate localized midlatitude exposures of water ice [*Combe et al*., 2016], as well as ammonia- and OH-bearing mineral phases distributed globally [*DeSanctis et al*., 2015]. VIR-MS data do not provide evidence for H_2O-bearing mineral phases at the surface, where phylosilicates, carbonates, and salts are likely desiccated by exposure to vacuum and sunlight. However, thermal evolution models [e.g., *Castillo-Rogez et al*., 2016], GRaND, and VIR-MS data collectively suggest that pit-forming volatiles can be sourced from both minerals and ice on Ceres. Which reservoir is dominant depends critically on the peak temperature of the brecciated layer in which pits develop.

Hydrodynamic impact models indicate that at the average impact speed among main belt asteroids (5 km/s) [*Marchi et al*., 2016], the material at the bottom of craters is heated to less than ~200–300 K [*Marchi et al*., 2013]. A small fraction of target material—namely, ejecta—is heated between ~300 K and ~800 K [*Marchi et al*., 2013]. Based on thermogravimetric analysis of meteorites [e.g., *Kolodny et al*., 1980; *Garenne et al*., 2014], CO_2 from carbonates is unlikely to be liberated in Cerean impact-heated material, due to its high temperature threshold for release (~1035 K). Hydroxides and hydroxyl groups in phyllosilicates can be liberated above ~473 K and ~673, respectively, and may make minor contributions to pit production. Molecular H_2O in the regolith (i.e., adsorbed water, water of hydration in salts, and crystalline ice) can readily vaporize at 300 K and above and likely dominates pit-forming volatile flows on Ceres. Ice may be the key player, given that crystalline ice is the only form of molecular H_2O that has been detected on Ceres' surface, and given that the regolith has a greater capacity to store H_2O as pore-space ice than as adsorbate and water of hydration.

On Mars, pitted crater materials are confined to middle and low latitudes; pit formation is thought to cease at high latitudes ($>50^{o}$) due to high ice concentrations [*Tornabene et al*., 2012; *Boyce et al*., 2012], which vary from ~50 to 100 vol.% [e.g., *Mellon et al*., 2009; *Feldman et al*., 2008]. Based on estimates of the total mass of H_2O that could be released from the pore space of a ~100 m brecciated layer, and on analogies with Mars, we conclude that the presence of pitted crater materials on Ceres places a rough upper limit on ice concentration in the target material of ~40–50 vol %. This upper limit is consistent with other lines of morphological evidence constraining ice content. The large-scale morphology of Cerean craters is

analogous to impact structures on icy satellites, indicating weak, ice-rich target materials [*Schenk*, 2015]; however, crater topography on Ceres persists over billion year timescales, indicating a significant silicate component to the upper crust and ice volume fractions <40% [*Bland et al*., 2016]. The association of Cerean pits with lobate ejecta and lobate mass wasting features much more extensive than those observed on Vesta also suggests a role for modest quantities of ice [*Scully et al*., 2015; *Hughson et al*., 2016; *Schmidt et al*., 2017]. Thus, pitted crater materials are strongly suggestive of ice in the Cerean regolith, and their presence at low and middle latitudes supports a theoretical paradigm in which shallow ice is present globally [*Fanale and Salvail*, 1989; *Schorghofer*, 2016], but ice is not a volumetrically dominant component of the upper meters to kilometers of the regolith [*Bland et al*., 2016; *Prettyman et al*., 2017].

The discovery of pitted impact materials on Mars, Vesta, and now Ceres suggests surprising similarities in postimpact surface modification on the three bodies. Similar pitted materials may be common in the asteroid belt. Understanding the distribution and abundance of volatiles, particularly water ice, in the regolith of rocky bodies will be of on-going interest for both astrobiology and in situ resource utilization. More detailed modeling of pit development processes is needed to elucidate the roles of impact temperature, volatile source, and volatile abundance in the formation of pitted impact materials in the inner solar system.

Acknowledgments
Portions of this work were supported by the Dawn at Ceres Guest Investigator Program, and by the Planetary Science Institute under contract with JPL, California Institute of Technology. The Dawn Mission is led by the University of California, Los Angeles, and is managed by JPL under the auspices of the NASA Discovery Program Office. Dawn data are archived with the NASA Planetary Data System (http://sbn.psi.edu/pds/archive/dawn.html).

References

Becker, K. J., R. W. Gaskell, L. LeCorre, and V. Reddy (2015), Hayabusa and Dawn image control from generation of digital elevation models for mapping and analysis, *Proc. Lunar Planet. Sci. Conf. 46th*, Abstract 2955.
Bland, M., et al. (2016), Composition and structure of the shallow subsurface of Ceres revealed by crater morphology, *Nat. Geosci., 9*, 538–542.
Blewett, D. T., et al. (2011), Hollows on Mercury: MESSENGER evidence for geologically recent volatile-related activity, *Science, 333,* 1856–1859.
Boyce, J. M., L. Wilson, P. J. Mouginis-Mark, C. W. Hamilton, and L. L. Tornabene (2012), Origin of small pits in martian impact craters, *Icarus, 221,* 262–275.
Buczkowski, D. L., et al. (2016a), Linear structures on Ceres: Morphology, orientation and possible formation mechanisms, *Proc. Lunar Planet. Sci. Conf. 47th*, Abstract 1262.
Buczkowski, D. L., et al. (2016b), The geomorphology of Ceres, *Science, 353,* doi:10.1126/science.aaf4332.
Byrne, S., and A. P. Ingersoll (2003), A sublimation model for Martian south polar ice features, *Science*, *299*, 1051–1053.
Capria, M. T., et al. (2014), Vesta surface thermal properties map, *Geophys. Res. Lett.*, *41*, 1438–1443, doi:10.1002/2013GL059026.
Castillo-Rogez, J. C., et al. (2016), Loss of Ceres' icy shell from impacts: Assessment and implications, *Proc. Lunar Planet. Sci. Conf. 47th*, Abstract 3012.
Combe, J.-Ph., et al. (2016), Detection of local H_2O exposed at the surface of Ceres, *Science*, *353*(6303), aaf3010.
Denevi, B. W., et al. (2012), Pitted terrain on Vesta and implications for the presence of volatiles, *Science, 338*, 246–249.
DeSanctis, M. C. et al. (2015), Ammoniated phyllosilicates with likely outer solar system origin on (1) Ceres, *Nature*, *528*, 241–244.
Fanale, F. P., and J. R. Salvail (1989), The water regime of asteroid (1) Ceres, *Icarus*, *82,* 97–110.
Feldman, W. C., M. T. Mellon, O. Gasnault, S. Maurice, and T. H. Prettyman (2008), Volatiles on Mars: Scientific results from the Mars odyssey Neutron Spectrometer, in *The Martian Surface: Composition, Mineralogy, and Physical Properties*, edited by J. F. Bell, pp. 125–148, Cambridge Univ. Press, London.
Garenne, A., P. Beck, G. Montes-Hernandez, R. Chiriac, F. Toche, E. Quirico, L. Bonal, and B. Schmitt (2014), The abundance and stability of "water" in type 1 and 2 carbonaceous chondrites (CI, CM and CR), *Geochim. Cosmochim. Acta, 137*, 93–112.
Heather, D. J., and S. K. Dunkin (2003), Geology and stratigraphy of king crater, lunar farside, *Icarus, 163,* doi:10.1016/S0019-1035(02)00063-5.
Hughson, K. H. G., et al. (2016), Hidden ice: Using aggregate spatial and physical properties of likely ground ice driven flows on Ceres to better understand its surface composition, *Geol. Soc. Am. Abstr. Programs*, *48*, 7, doi: 10.1130/abs/2016AM-281111.
Kneissl, T., S. van Gasselt, and G. Neukum (2011), Map-projection-independent crater size-frequency determination in GIS environments – New software tool for ArcGIS, *Planet. Space Sci., 59,* 1243–1254.
Kolodny, Y. J. F. Kerridge, and I. R. Kaplan (1980), Deuterium in carbonaceous Chondrites, *Earth Planet. Sci. Lett., 46*, 149–158.
Malin, M. C., and K. S. Edgett (2001), Mars Global Surveyor Mars orbiter Camera: Interplanetary cruse through primary mission, *J. Geophys. Res., 110,* 23,429–23,570.
Malin, M. C., M. A. Caplinger, and S. D. Davis (2001), Observational evidence for an active surface reservoir of solid carbon dioxide on Mars, *Science, 294,* 2146–2148.
Mangold, N. (2011), Ice sublimation as a geomorphic process: A planetary perspective, *Geomorphology*, *126*, 1–17.
Marchi, S., et al. (2013), High-velocity collisions from the lunar cataclysm recorded in asteroidal meteorites, *Nat. Geosci., 6,* 303–307.
Marchi, S., et al. (2016), The missing large impact craters on Ceres, *Nat. Commun.*, *7*, doi:10.1038/ncomms12257.
McCord, T. B., and C. Sotin (2005), Ceres: Evolution and current state, *J. Geophys. Res.*, *110*, E05009, doi:10.1029/2004JE002244.
McEwen, A. S., et al. (2007), A closer look at water-related activity on Mars, *Science*, *317*, 1706–1709.
Mellon, M. T., et al. (2009), Ground ice at the phoenix landing site: Stability state and origin, *J. Geophys. Res., 114,* E00E07, doi: 10.1029/2009JE003417.
Milliken, R. E., and J. F. Mustard (2003), Erosional morphologies and characteristics of latitude-dependent surface mantles on Mars, *Sixth International Conference on Mars*, Abstract 3240.
Morris, A., P. J. Mouginis-Mark, and H. Garbeil (2010), Possible impact melt and debris flows at Tooting crater, Mars, *Icarus, 209,* 369–389.
Moore, J. M., M. T. Mellon, and A. P. Zent (1996), Mass wasting and ground collapse in terrains of volatile-rich deposits as a solar system-wide geological process: The pre-Galileo view, *Icarus, 122,* 63–78.
Mouginis-Mark, P. J., and H. Garbeil (2007), Crater geometry and ejecta thickness of the Martian impact crater Tooting, *Meteorit. Planet. Sci. 42*, 1615–1625.
Preblich, B., A. McEwen, and D. Studer (2007), Mapping rays and secondary craters from Zunil, Mars, *J. Geophys. Res., 112,* E05006, doi:10.1029/2006JE002817.

Prettyman, T. H., et al. (2017), Extensive water ice within Ceres' aqueously altered regolith: Evidence from nuclear spectroscopy, *Science, 355,* 55–59, doi:10.1126/science.aah6765.
Preusker, F., et al. (2016), Dawn at Ceres—Shape model and rotational state, *Proc. Lunar Planet. Sci. Conf. 47th*, Abstract 1954.
Reddy, V., et al. (2012), Color and albedo heterogeneity of Vesta from Dawn, *Science*, *336,* doi:10.1126/science.1219088.
Rivkin, A. S., et al. (2010), The surface composition of Ceres, *Space Sci. Rev. 163*, 95–116.
Schenk, P. (2015), An ice-rich mantle on Ceres from Dawn mapping of central pit and peak crater morphologies, Abstract P53E-2186 presented at 2015 Fall Meeting, AGU, San Francisco, Calif.
Schmidt, B. E., et al. (2017), Geomorphological evidence for ground ice on dwarf planet Ceres, *Nat. Geosci.*, *10*, 338–343, doi:10.1038/ngeo2936.
Schorghofer, N. (2008), The lifetime of ice on main belt asteroids, *Ap. J., 682,* 697–705.
Schorghofer, N. (2016), Predictions of depth-to-ice on asteroids based on an asynchronous model of temperature, impact stirring, and ice loss, *Icarus*, *276*, 88–95.
Schmedemann, N., et al. (2017), Timing of optical maturation of recently exposed material on Ceres, *Geophys. Res. Lett.*, *43*, 11,987–11,993, doi:10.1002/2016GL071143.
Scully, J. E. C., C. T. Russell, A. Yin, R. Jaumann, E. Carey, J. Castillo-Rogez, H. Y. McSween, C. A. Raymond, and V. Reddy (2015), Geomorphological evidence for transient water flow on Vesta, *Earth Planet. Sci. Lett., 411*, 151–163.
Tosi, F., et al. (2014), Thermal measurements of dark and bright surface features on Vesta as derived from Dawn/VIR, *Icarus*, *240*, 36–57.
Tornabene, L. L., et al. (2006), Identification of large (2–10 km) rayed craters on Mars in THEMIS thermal infrared images: Implications for possible Martian meteorite source regions, *J. Geophys. Res.*, *111*, E10006, doi:10.1029/2005JE002600.
Tornabene, L. L., et al. (2007), Impact melting and the role of subsurface volatiles: Implications for the formation of valley networks and phyllosilicate-rich lithologies on early Mars, in *International Conf. on Mars VII. Lunar Planet. Sci. Inst. Contri. No. 1353*.
Tornabene, L. L., G. R. Osinski, A. S. McEwen, J. M. Boyce, V. J. Bray, C. M. Caudill, J. A. Grant, C. W. Hamilton, S. Mattson, and P. J. Mouginis-Mark (2012), Widespread crater-related pitted materials on Mars: Further evidence for the role of target volatiles during the impact process, *Icarus, 220,* 348–368.
Williams, D. A., et al. (2017), The geology of the Kerwan quadrangle of dwarf planet Ceres: Investigating Ceres' oldest impact basin, *Icarus,* doi:10.1016/j.icarus.2017.05.004.